



Density of states in the tight binding model

Juan Luis Verbena

Supervisor: Dr. Stoyan Jelev Vlaev

For the degree of Bachelor in Physics

Universidad Autónoma de Zacatecas

September 2007

Abstract

Here we present an original method for obtaining the density of states in the tight binding model.

We offer an introduction in the first chapter.

In the second chapter we develop the theoretical basis of the tight binding model according to Green's functions. We start out with Bloch's theorem and formulate the semi-empirical method of the tight binding model, with which we'll work out the dispersion relations.

In the third chapter we describe the density of states, its definition from quantum mechanics and its application to the tight binding model. We end the chapter with the formulas used to calculate the density of states for one, two and three dimensional crystals.

In the fourth chapter we describe the program we have used and we make a historical review description of the integration over the Brillouin Zone.

Finally we present the results obtained for one, two and three dimensions. Also we show the results obtained if we change the order of integration and extraction of the imaginary part.

Resumen

En el presente trabajo se presenta un método original para calcular la densidad de estados en el modelo de enlace fuerte.

En el primer capítulo ofrecemos una introducción.

En el segundo capítulo desarrollamos las bases teóricas del modelo de enlace fuerte en el esquema de las funciones de Green. Comenzamos con el teorema de Bloch y formulamos el método semiempírico de enlace fuerte, modelo con el que trabajamos para encontrar las relaciones de dispersión.

En el tercer capítulo describimos la densidad de estados, su definición de la mecánica cuántica y la aplicación al modelo de enlace fuerte. Finalizamos describiendo las fórmulas para encontrar la densidad de estados para cristales uni, bi y tridimensionales.

En el cuarto capítulo se habla sobre el programa utilizado para integrar funciones complejas singulares y se hace una revisión de los antecedentes sobre la integración sobre la zona de Brillouin.

Finalmente se presentan los resultados que hemos obtenido para cristales de una, dos y tres dimensiones. También se presenta un resultado interesante que se obtiene al cambiar el orden de cálculo de la integración y de la extracción de la parte imaginaria.

Contents

Contents	i
List of Figures	ii
1 Introduction	1
2 Bloch's theorem, tight binding and Green's functions	3
2.1 Description of the semi-empirical tight binding model	3
2.1.1 Bloch's theorem for uni-dimensional periodicity	3
2.1.2 The tight binding method	6
2.1.3 Semiempirical frame of tight binding	7
2.2 Dispersion laws for ideal crystals 1D, 2D and 3D	8
3 Density of states	13
3.1 Introduction: Properties of matter	13
3.2 Definition from quantum mechanics	13
3.2.1 Density of states and Green's functions	13
3.3 DOS for 1D, 2D and 3D crystals	15
4 Numerical integration of discontinuous functions	19
4.1 Numerical integration with MATHEMATICA	19

4.1.1	The NINTEGRATE command	19
4.1.2	MATHEMATICA's integration methods	20
4.2	Special points to average over the Brillouin zone	22
4.3	Background	23
4.3.1	Evolution in the calculation of integrals in the Brillouin zone	23
5	Results and Discussion	33
5.1	1D	33
5.2	2D	34
5.3	3D	34
5.4	Change of the order of the calculations	36
5.5	Conclusion	37
	Bibliography	39

List of Figures

2.1	Chain of three atoms.	8
2.2	Schematical representation of the potential of a crystal as the superposition of similar potentials to the atoms centered in positions in the lattice t_n . In the tight binding approximation, the interaction between atomic orbitals ϕ_a of energy E_a lead to the formation of energy bands.	9
4.1	Density of states with $\gamma = s = 0.1$, integrated by the Gauss-Kronrod (left) and Double exponential (right) method. At the bottom is the time taken. .	20
4.2	Density of states with $\gamma = s = 0.1$, integrated by the trapezoidal (left) and Monte Carlo (right) method. At the bottom is the time taken.	21
4.3	Density of states with $\gamma = s = 0.1$, integrated by the Monte Carlo method. At the bottom is the time taken.	21
4.4	Coordinates of the mean value point for several geometries. From Baldereschi (1973).	24
4.5	Bidimensional Brillouin zones and their irreducible segments for the five types of lattice: oblicuous, centered rectangular, primitive rectangular, square, and hexagonal, from Cunningham (1974).	25
4.6	Solid angle integrals approximated to integrals over triangles. From Holas (1976).	26

4.7	Integrals of the Green's functions for the simple cubic tight binding band. The number of tetrahedroes used in the integration is 1728 for the linear case, and 216 in the quadratic case. From Boon, Methfessel & Mueller (1986).	27
4.8	k points spaced in irreducible segments. From Wieseneker (1987).	28
4.9	Generalized cones of Boerrigter (1988). In the upper left image we show a generalized cone surrounding an atom in position R. The plane has four plane edges. In the upper right figure it is shown an integration region made of a square base piramid. In the lower figure we can see the integration region consisting of a triangular based piramid, or "simplex".	29
4.10	The error in the weight factors is shown. In the upper part of each square, we see the factor as considered by Winkler (1993) and in the bottom the one considered by the quadratic interpolation scheme. From Winkler (1993).	30
5.1	Routine that calculates the density of states for an infinite chain.	33
5.2	Plots of the density of states for an infinite chain with varying parameters.	34
5.3	Routine that calculates the density of states for a square lattice.	35
5.4	Plots of the density of states for a square lattice with varying parameters.	35
5.5	Routine that calculates the density of states for a cubical lattice.	35
5.6	Plots of the density of states for a cubical lattice with varying parameters.	36
5.7	Curves we obtained integrating just the imaginary part. We can see some noise that doesn't show when we first integrate and then separate.	37

Chapter 1

Introduction

The density of states (DOS) is the main characteristic of any quantum mechanical system. In the physics of condensed matter, the DOS is usually obtained via an integration over the first Brillouin zone. Single, double and triple integrals need to be solved if we work on 1D, 2D or 3D systems, respectively. The variables in any case are the components of the electron's wave vector in its movement through the periodic crystal. The integrands are the local density of states (LDOS). The DOS, by definition, depends only on the energy, while the LDOS depends also on the variable \mathbf{k} .

In homogeneous ideal crystals, calculating the DOS requires integration of singular functions in the reciprocal space of the vector \mathbf{k} , which makes the numerical calculation much more difficult than the integration of continuous functions. In the literature we can find methods that deal with singular integrals.

In contemporary solid state physics great attention is given to systems of low dimensionality due to their applications in nanotechnology, quantum dots, quantum threads and plane heterostructures (quantum wells and superlattices) possess physical properties (microscopical and macroscopical) because of the fundamental physical parameter: dimensionality, which will be 0D, 1D and 2D for quantum dots, threads, and wells and

superlattices. Systems of reduced dimensionality preserve periodicity in one or two variables and lose it in two or one, respectively, in three in the case of quantum dots. In the context of nanostructures, the computation of the DOS has its peculiarities. One of the main tasks in the theory of systems of low dimensionality is numerical and analytical (in the few cases where this can be done) calculations of the DOS for real materials. The purpose of the present work is to make use of the tools offered by MATHEMATICA to integrate singular functions related to the DOS.

Chapter 2

Bloch's theorem, description of the tight binding model and the Green's function method

2.1 Description of the semi-empirical tight binding model

2.1.1 Bloch's theorem for uni-dimensional periodicity

We have Schrödinger's equation:

$$-\frac{\hbar^2}{2m} \frac{d^2\Psi(x)}{dx^2} + V(x)\Psi(x) = E\Psi(x) \quad (2.1)$$

And we know several solutions for typical potentials $V(x)$. Here $V(x)$ is a periodic potential of a unidimensional crystal lattice with lattice constant \mathbf{a} .

The potential satisfies:

$$V(x) = V(x + ma) \quad (2.2)$$

i.e. it's a periodic potential.

Fourier's transform of a periodic potential $V(x)$ includes only plane waves with wave numbers:

$$h_n = n \frac{2\pi}{a} \quad (2.3)$$

So we see that Fourier spectrum is discrete. We are interested in the eigenvalues and eigenfunctions. In the case of a free electron, the plane wave functions are described as follows:

$$w_k(x) = \frac{1}{\sqrt{L}} e^{ikx} \quad (2.4)$$

Equation 2.4 is normalized to 1 when $0 \leq x \leq L$ where L is the length of the crystal.

Now, going back to the eigenvalues of 2.1, where we have a periodic potential that satisfies 2.2, when we apply the operator:

$$H = \frac{p^2}{2m} V(x) \quad (2.5)$$

To the plane wave w_k we see that $H(V(x))$ belongs to the subspace S_k of plane waves with wave numbers $k + h_n$:

$$S_k \equiv \{W_k(x), W_{k+h_1}(x), W_{k-h_1}(x), W_{k+h_2}(x), W_{k-h_2}(x) \dots\} \quad (2.6)$$

This subspace is closed under the operation of applying H to any of its elements.

S_k and $S_{k'}$ are different only if k and k' are not related by a factor of $2h/a$.

They are the same any other way. So we can define the Brillouin zone as the zone in

space bounded by:

$$-\frac{\pi}{a} < k \leq \frac{\pi}{a} \quad (2.7)$$

This includes all the different k 's that yield independent subspaces S_k .

Any generic wave function $\Psi_k(x)$ obtained via diagonalization of H in subspace S_k can be expressed by an appropriate linear combination, like the one shown below:

$$\Psi_k(x) = \sum_n C_n(k) \frac{1}{\sqrt{L}} e^{i(k+h_n)x} \quad (2.8)$$

For convenience we re-write:

$$u_k(x) = \sum_n C_n(k) \frac{1}{\sqrt{L}} e^{ih_n x} = \sum_n C_n(k) \frac{1}{\sqrt{L}} e^{in(\frac{2\pi}{a})x} \quad (2.9)$$

This way:

$$\Psi_k(x) = e^{ikx} u_k(x) \quad (2.10)$$

$u_k(x)$ is a periodic function. Equation 2.9 expresses the following: **any physically acceptable solution of Schrödinger's equation in a periodic potential takes the form of a travelling wave modulated at a microscopic scale by an appropriate function of the periodicity of the lattice.**

$$\Psi_k(x + t_n) = e^{ik(x+t_n)} u_k(x + t_n) = e^{ik(x+t_n)} u_k(x) = e^{ikx} e^{ikt_n} u_k(x) = e^{ikt_n} \Psi_k(x) \quad (2.11)$$

$$\Psi_k(x + t_n) = e^{ikt_n} \Psi_k(x) \quad (2.12)$$

Which is Bloch's theorem. Note that 2.10 implies 2.12 and viceversa.

2.1.2 The tight binding method

The tight binding method suggested by Bloch in 1928 consists of expanding the states of the crystal in linear combinations of atomic orbitals of the component atoms. This method provides a reasonable description of the occupied states in any kind of crystal and also of the lower conduction states.

We start by considering a simple crystal with an atom per unitary cell. Then $\phi_i(r)$ is an atomic orbital of quantum number i and energy E_i of the atom centered in the unitary cell t_m . We construct a Bloch sum; that is, a linear combination that satisfies Bloch's theorem.

$$\phi_i(k, r) = \frac{1}{\sqrt{N}} \sum_{t_m} e^{ikt} \phi(r - t_m) \quad (2.13)$$

Where $\phi_i(r)$ is the same orbital for the atom in the unitary cell t_m . N is the number of unitary cells in the crystal.

A number of Bloch's sums are used to expand the wave functions of the crystal:

$$\Psi(k, r) = \sum_i C_i(k) \phi_i(k, r) \quad (2.14)$$

The coefficients C_i are determined by variational methods. Applying the variational principle we see that the eigenvalues and the eigenfunctions are obtained from:

$$||M_{ij}(k) - ES_{ij}(k)|| = 0 \quad (2.15)$$

Where $M_{ij}(k)$ are matrix elements of the crystal's hamiltonian amongst Bloch's sums and $S_{ij}(k)$ are interlacing matrix elements.

$$M_{ij}(k) = \langle \phi_i(k, r) | H | \phi_j(k, r) \rangle \quad (2.16)$$

$$S_{ij}(k) = \langle \phi(k, r) | \phi_j(k, r) \rangle \quad (2.17)$$

These are to be evaluated numerically, performing the appropriate integrals in any unitary cell in real space.

2.1.3 Semiempirical frame of tight binding

Working on this frame we make some drastic assumptions about the matrix elements of the hamiltonian and about the interaction between atoms.

First, we can see that, in the case of extremely localized atomic orbitals, the bulking of atomic functions centered on different atoms becomes negligible. This justifies the assumption that the localized atomic orbitals are orthonormal and therefore also the corresponding Bloch sums, $S_{ij}(k) \rightarrow \delta_{ij}$.

$$M_{ij}(k) = \langle \phi_i(k, r) | H | \phi_j(k, r) \rangle \quad (2.18)$$

$$M_{ij}(k) = \frac{1}{\sqrt{N}} \sum_{t_m} e^{-ik \cdot t_m} \langle \phi_i(r - t_m) | H | \phi_j(k, r) \rangle \quad (2.19)$$

$$M_{ij}(k) = \frac{1}{N} \sum_{t_m, t_n} e^{-ik \cdot t_m} e^{ik \cdot t_n} \langle \phi_i(r - t_m) | H | \phi_i(r - t_n) \rangle \quad (2.20)$$

$$M_{ij}(k) = \frac{1}{N} \sum_{t_m, t_n} e^{ik \cdot (t_n - t_m)} \langle \phi_i(r - t_m) | H | \phi_i(r - t_n) \rangle \quad (2.21)$$

H is invariant to translation, thus we have $t_m = 0$:

$$M_{ij}(k) = \sum_{t_n} e^{ik \cdot t_n} \langle \phi_i(r) | H | \phi_i(r - t_n) \rangle \quad (2.22)$$

In semi-empirical evaluations it is convenient to express the potential of the crystal as



Figure 2.1: Chain of three atoms.

a sum of spherically symmetric atomic potentials $V_a(r - t_n)$ centered in positions in the lattice.

2.2 Dispersion laws for ideal crystals 1D, 2D and 3D

We take an hypothesis to explain energy bands: we imagine the construction of a crystal from a hypothetical, unidimensional, periodic sequence of similar atoms.

There is interaction between these N atoms, this way the degeneration of N interacting atoms is removed and evolves into an energy band.

The distance from atom to atom is a . In figure 2.2 we can see identical atoms with the same in-between spaces. The position of each of the atoms will be given, naturally, by $t_n = na$. For each of the atoms we concentrate on a local given orbit ϕ_a of energy E_a (we assume ϕ_a is not degenerate and it is in real form).

It is convenient to represent the hamiltonian of the crystal H in the localized functions $\{\phi_a(x - t_n)\}$. We wish to exploit the translational symmetry of the hamiltonian. The diagonal elements are all the same, also, the jump integrals between first neighbors are the same.

$$\langle \phi_a(x - t_n) | H | \phi_a(x - t_n) \rangle = E_0 \quad (2.23)$$

$$\langle \phi_a(x - t_n) | H | \phi_a(x - t_n \pm 1) \rangle = \gamma \quad (2.24)$$

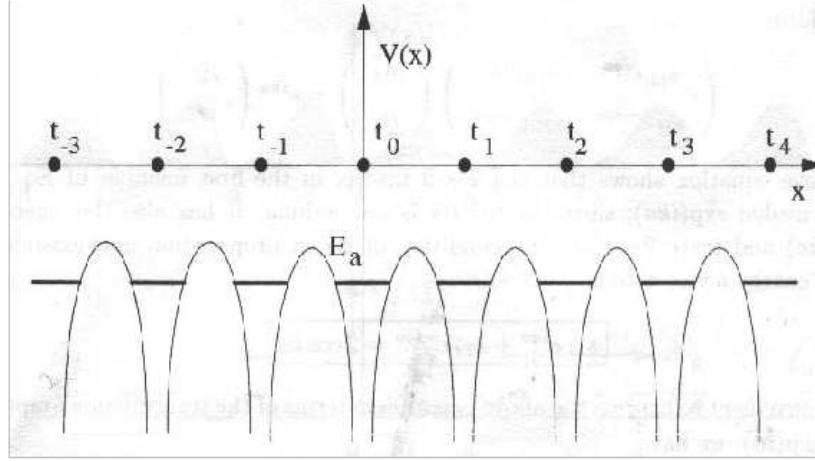


Figure 2.2: Schematic representation of the potential of a crystal as the superposition of similar potentials to the atoms centered in positions in the lattice t_n . In the tight binding approximation, the interaction between atomic orbitals ϕ_a of energy E_a lead to the formation of energy bands.

For simplicity, we ignore all the integrals that involve second neighbors and so on. The value of γ is considered negative to simulate the case of type s orbitals and an attractive atomic potential.

Since the functions $\{\phi_a(x - t_n)\}$ do not satisfy Bloch's theorem, we will remedy this by considering a linear combination of atomic orbitals as:

$$\phi(k, x) = \frac{1}{\sqrt{N}} \sum_{t_n} e^{ikt_n} \phi_a(x - t_n) \quad (2.25)$$

N is the number of unitary cells in the crystal.

For simplicity we assume also orthonormality of the orbitals centered in different atoms, so that Bloch's sums are also orthonormal. The N itinerant Bloch's sums $\{\phi(k, x)\}$ represent the same Hilbert's space as the N localized functions $\{\phi_a(x - t_n)\}$. Bloch's sums for different k 's cannot be mixed under the influence of a periodic potential.

The energy dispersion of an energy band originated from the atomic orbitals $\{\phi_a(x -$

$t_n)\}$ will be given by:

$$E(k) = \langle \phi(k, x) | H | \phi(k, x) \rangle \quad (2.26)$$

For a unidimensional crystal:

$$E(k) = \frac{1}{N} \sum_{t_n, t_m} e^{ik(t_m - t_n)} \langle \phi_a(x - t_n) | H | \phi_a(x - t_m) \rangle \quad (2.27)$$

Due to the translational symmetry, that is, that from any part of the crystal we see the same, we eliminate one of the sum indexes, obtaining.

$$E(k) = \frac{1}{N} \sum_{t_n} e^{ik(t_m - t_n)} \langle \phi_a(x - t_n) | H | \phi_a(x - t_m) \rangle \quad (2.28)$$

Given the approximation to first neighbors, we have the following three cases:

$$t_m - t_n = 0 \quad (2.29)$$

$$t_m - t_n = 1$$

$$t_m - t_n = -1$$

Exposing the three terms of the sum explicitly.

$$\begin{aligned} E(k) = & \langle \phi_a(x - t_n) | H | \phi_a(x - t_n) \rangle + e^{ik} \langle \phi_a(x - t_n) | H | \phi_a(x - t_n - 1) \rangle \\ & + e^{-ik} \langle \phi_a(x - t_n) | H | \phi_a(x - t_n + 1) \rangle \end{aligned} \quad (2.30)$$

And using 2.25:

$$E(k) = E_0 + \gamma(e^{ik} + e^{-ik}) \quad (2.31)$$

$$E(k) = E_0 + 2\gamma \cos k \quad (2.32)$$

2.32 is the dispersion relation for a unidimensional crystal.

This relation can be expanded for bidimensional and tridimensional crystals.

So we have for two and three dimensions respectively.

$$E(k_x, k_y) = E_0 + 2\gamma(\cos k_x + \cos k_y) \quad (2.33)$$

$$E(k_x, k_y, k_z) = E_0 + 2\gamma(\cos k_x + \cos k_y + \cos k_z) \quad (2.34)$$

Chapter 3

Density of states

3.1 Introduction: Properties of matter

A solid is made up of a series of atoms that form a compact set. The proximity between the atoms is responsible for the characteristic properties of this state of matter. The ionic bond and covalent bond, responsible for the formation of molecules, have an important representation in the solid state. The **Van der Waals'** force and the metallic bond give place, respectively, to the constituent cohesion forces of molecular crystals and metals. These bonds are of electrostatic origin, so that the main distinction between them would be in the positioning of the electrons around the atoms and the molecules, that make up the crystalline lattice.

3.2 Definition from quantum mechanics

3.2.1 Density of states and Green's functions

We consider a system described by a hamiltonian H , and indicate Ψ_m and E_m as its normalized eigenfunctions and eigenvalues. We define:

$$D(E) = \sum_m \delta(E - E_m) \quad (3.1)$$

As the total density of states.

The density of states, projected over an arbitrarily chosen state of interest $|f_0\rangle$, normalized to unity is defined as:

$$n_0(E) = \sum_m |\langle f_0 | \Psi_m \rangle|^2 \delta(E - E_m) \quad (3.2)$$

The total density of states is the sum of the density of states projected over a full orthonormal set f_n . The retarded Green's function of H is defined as:

$$G(E + is) = \frac{1}{E + is - H} \quad (3.3)$$

Green's function is connected to the density of states of the function. We consider, for example, a diagonal matrix element of Green's function, for example:

$$G_{00}(E + is) = \langle f_0 | \frac{1}{E + is - H} | f_0 \rangle \quad (3.4)$$

$$G_{00}(E + is) = \langle f_0 | \sum_m |\Psi_m\rangle \langle \Psi_m | \frac{1}{E + is - H} | f_0 \rangle \quad (3.5)$$

$$G_{00}(E + is) = \sum_m |\langle f_0 | \Psi_m \rangle|^2 \frac{1}{E + is - E_m} \quad (3.6)$$

$$G_{00}(E + is) = \sum_m |\langle f_0 | \Psi_m \rangle|^2 \frac{E - E_m - is}{(E - E_m)^2 + s^2} \quad (3.7)$$

Where we have introduced the identity operator.

The real part exhibits poles that correspond to the discrete eigenvalues of H . The imaginary part shows type δ singularities. We can see this using:

$$\lim_{s \rightarrow 0} \frac{1}{\pi} \frac{s}{(E - E_m)^2 + s^2} = \delta(E - E_m) \quad (3.8)$$

From 3.2, 3.7 and 3.8, we obtain the **standard spectral theorem**:

$$n_0(E) = \sum_m |\langle f_0 | \Psi_m \rangle|^2 \delta(E - E_m) \quad (3.9)$$

$$n_0(E) = \sum_m |\langle f_0 | \Psi_m \rangle|^2 \lim_{s \rightarrow 0} \frac{1}{\pi} \frac{s}{(E - E_m)^2 + s^2} \quad (3.10)$$

$$n_0(E) = -\frac{1}{\pi} \lim_{s \rightarrow 0} \Im G_{00}(E + is) \quad (3.11)$$

From here it follows that the total density of states can be expressed as the trace of any orthonormal set's Green's function.

$$D(E) = -\frac{1}{\pi} \lim_{s \rightarrow 0} \Im \text{Tr} G_{00}(E + is) \quad (3.12)$$

From 3.12 we obtain the expressions that we will use to calculate the DOS.

$$D(E) = -\frac{1}{\pi} \Im \int_{-\frac{\pi}{a}}^{\frac{\pi}{a}} G(E + is; k) dk \quad (3.13)$$

With Green's function defined as:

$$G(E + is; k) = \frac{1}{E + is - H} = \frac{1}{E + is - E(k)} \quad (3.14)$$

Which is an integral over the Brillouin zone, therefore the integration limits. Depending on the dimensionality of the crystal the integral will be 1D, 2D or 3D.

3.3 DOS for 1D, 2D and 3D crystals

Now we show the formulas that will be used to obtain the DOS. In the next formulas E is the energy of the system, K, k_x, k_y, k_z are wave vectors, a is the lattice constant, s is the small imaginary part of the energy, according to the theory of complex variable and

Green's functions, and γ is the parameter of the interaction between two atoms that are first neighbors.

The Brillouin zone of the reciprocal space is described for one, two, or three dimensions respectively.

$$\begin{aligned}
 \text{1D} \quad k &= \left\{-\frac{\pi}{a}, \frac{\pi}{a}\right\} \\
 \text{2D} \quad k_x &= \left\{-\frac{\pi}{a}, \frac{\pi}{a}\right\} \quad k_y = \left\{-\frac{\pi}{a}, \frac{\pi}{a}\right\} \\
 \text{3D} \quad k_x &= \left\{-\frac{\pi}{a}, \frac{\pi}{a}\right\} \quad k_y = \left\{-\frac{\pi}{a}, \frac{\pi}{a}\right\} \quad k_z = \left\{-\frac{\pi}{a}, \frac{\pi}{a}\right\}
 \end{aligned} \tag{3.15}$$

For and **infinite chain**:

The dispersion law, Green's function and density of states, respectively:

$$E(k) = E_0 + 2\gamma \cos k \tag{3.16}$$

$$G_{1D}(E + is; k) = \frac{1}{E + is - E_0 - 2\gamma \cos ka} \tag{3.17}$$

$$D_{1D}(E) = -\frac{1}{\pi} \Im \int_{-\frac{\pi}{a}}^{\frac{\pi}{a}} G_{1D}(E + is; k) dk \tag{3.18}$$

For the **square lattice**:

The dispersion law, Green's function and density of states, respectively:

$$E(k_x, k_y) = E_0 + 2\gamma(\cos k_x a + \cos k_y a) \tag{3.19}$$

$$G_{2D}(E + is; k_x, k_y) = \frac{1}{E + is - E_0 - 2\gamma(\cos k_x a + \cos k_y a)} \tag{3.20}$$

$$D_{2D}(E) = -\frac{1}{\pi} \Im \int_{-\frac{\pi}{a}}^{\frac{\pi}{a}} G_{2D}(E + is; k_x, k_y) dk \tag{3.21}$$

For the **simple cubic lattice**:

$$E(k_x, k_y, k_z) = E_0 + 2\gamma(\cos k_x a + \cos k_y a + \cos k_z a) \quad (3.22)$$

$$G_{3D}(E + is; k_x, k_y, k_z) = \frac{1}{E + is - E_0 - 2\gamma(\cos k_x a + \cos k_y a + \cos k_z a)} \quad (3.23)$$

$$D_{3D}(E) = -\frac{1}{\pi} \Im \int_{-\frac{\pi}{a}}^{\frac{\pi}{a}} G_{3D}(E + is; k_x, k_y, k_z) dk \quad (3.24)$$

Making use of these formulas and setting, for simplicity, the parameter $a = 0$, we can make the calculations shown in the following chapter.

Chapter 4

Numerical integration of discontinuous functions

4.1 Numerical integration with MATHEMATICA

4.1.1 The NINTEGRATE command

Numerical integration is important due to the relatively small number of functions that can be integrated exactly. The command

`NIntegrate[integrand, {x, x0, x1}, options]`

calculates a numerical approximation to the integral:

$$\int_{x_0}^{x_1} \text{integrand} \, dx \tag{4.1}$$

For the calculation of integrals over line segments in the complex plane we use the notation:

$\{x, x_{\text{start}}, x_{\text{between}_1}, x_{\text{between}_2}, \dots, x_{\text{between}_n}, x_{\text{end}}\}$

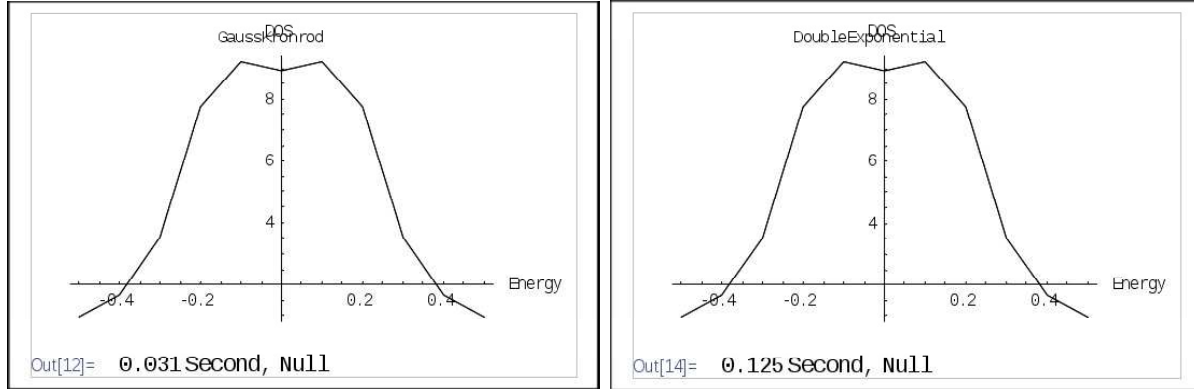


Figure 4.1: Density of states with $\gamma = s = 0.1$, integrated by the Gauss-Kronrod (left) and Double exponential (right) method. At the bottom is the time taken.

A similar notation can be used to indicate points where singularities may occur.

By making use of MATHEMATICA, we can calculate integrals with integrable singularities by a change of variable, which isn't visible to the user, for example:

```
NIntegrate[1/Sqrt[x], {x, 0, 1}]
```

4.1.2 MATHEMATICA's integration methods

The methods we can find in MATHEMATICA for our numerical integration are the following: *Gausskronrod*, *Doubleexponential*, *Trapezoidal*, *Montecarlo*, *Quasimontecarlo*. In figures 4.1-4.3 we show the different times each method takes in the same integration with parameters: $\gamma = s = 0.1$. We can also see this information in table 4.1.

Table 4.1: Time the integration took for the different integration methods ordered by speed.

Method of integration	Time it took (seconds)
Trapezoidal	0.016
Gauss-Kronrod	0.031
Double Exponential	0.125
Montecarlo	0.563
Quasi Montecarlo	0.703

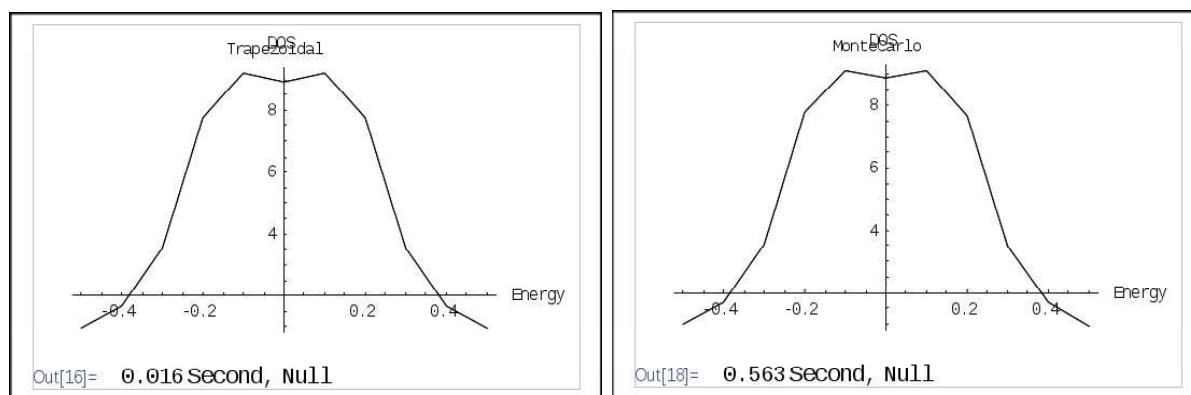


Figure 4.2: Density of states with $\gamma = s = 0.1$, integrated by the trapezoidal (left) and Monte Carlo (right) method. At the bottom is the time taken.

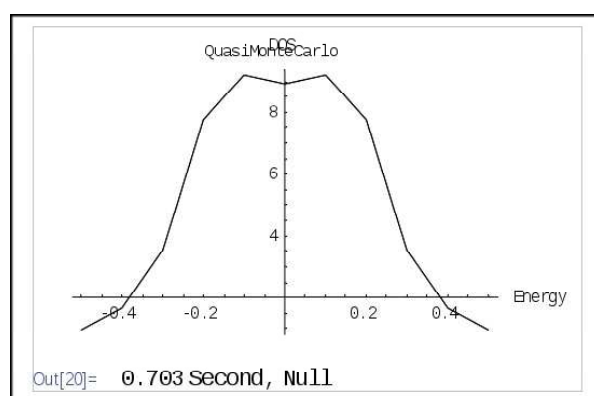


Figure 4.3: Density of states with $\gamma = s = 0.1$, integrated by the Monte Carlo method. At the bottom is the time taken.

4.2 Special points to average over the Brillouin zone

In Baldereschi (1973) the average of a function over the Brillouin zone is defined as:

$$F_0 = \frac{1}{N} \sum_k^{\text{BZ}} F(k) \quad (4.2)$$

So that F_0 is the average value of the function $F(k)$. N is the number of allowed k vectors in the Brillouin zone.

To understand the basic principles about special points let's consider a function:

$$F(k) = F_0 + \sum_{t_n \neq 0} F_n e^{ikt_n} \quad (4.3)$$

In several situations of physical interest, the Fourier coefficients in 4.3 depend only on $|t_n|$, in these cases we express 4.3 in the following way:

$$F(k) = F_0 + F_1 \sum_{t_i^{(1)}} e^{ikt_i^{(1)}} + F_2 \sum_{t_i^{(2)}} e^{ikt_i^{(2)}} + F_3 \sum_{t_i^{(3)}} e^{ikt_i^{(3)}} + \dots \quad (4.4)$$

Where $t_i^{(1)}$ is the first shell of neighboring traslation vectos, $t_i^{(2)}$, is the second one, and so forth. For instance, we would have six vectors for the first shell: $(\pm a, 0, 0)$, $(0, \pm a, 0)$, $(0, 0, \pm a)$.

For the second shell eleven vectors. $(\pm a, \pm a, 0)$, $(\pm a, 0 \pm a)$, $(0, \pm a, \pm a)$.

And eight for the third shell: $(\pm a, \pm a, \pm a)$. So that 4.4 turns into:

$$\begin{aligned} F(k) = & F_0 + 2F_1(\cos k_x a + \cos k_y a + \cos k_z a) + \\ & 4F_2(\cos k_x a \cos k_y a + \cos k_x a \cos k_z a + \cos k_y a \cos k_z a) + \\ & 8F_3(\cos k_x a \cos k_y a \cos k_z a) \end{aligned} \quad (4.5)$$

This way we can see there is a point (Baldereschi's point) that reduces to zero the contributions from the first, second and third shells:

$$k = \frac{\pi}{2} \left(\frac{1}{2}, \frac{1}{2}, \frac{1}{2} \right) \quad (4.6)$$

This is called **mean value point**.

4.3 Background

4.3.1 Evolution in the calculation of integrals in the Brillouin zone

Introduction

Integrals in the Brillouin zone are singular most of the time, which makes them difficult to calculate, so that it is necessary to use numerical methods instead of analytical. Also, the way this calculations are performed has been evolving as we discover mathematical details that make this a less complicated task.

These integrals are very important in condensed matter physics: there exist characteristic information on solids that can only be obtained by means of these integrals. For example the density of states, a fundamental parameter of a solid. It'll provide us with information about the energy levels of the material.

Due to the importance of singula integrals in solid state physics, we present a discussion about the optimization of this calculation.

I

In 1973, Baldereschi introduces a new special point, which he called mean value point. In Baldereschi (1973) he notes how useful this point can be for computing singular integrals,

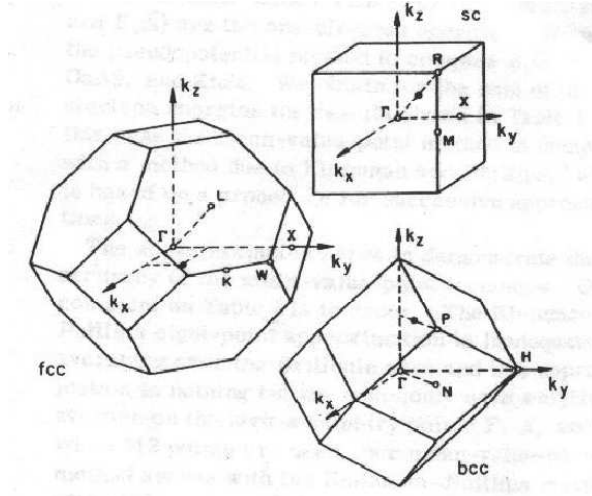


Figure 4.4: Coordinates of the mean value point for several geometries. From Baldereschi (1973).

since these were performed around a random quantity of points also random, and then this values were averaged, until Chadi & Cohen proposed the existence of special points that made this computations easier, eliminating the need for such a big number of points as was usually used. Baldereschi then found a new point, which he called the mean value point because the value that any function could take in the point is the same or an excelent approximation to the average value of the function evaluated over the whole Brillouin zone.

Baldereschi then defines the mean value point as a point in which any periodic function of the wave vector takes an excelent approximation to the average value of the same function over the whole Brillouin zone. He also obtained the coordinates of this points for cubic meshes. This points have a stron dependence on thne symmetry of the crystal under study.

In figure 4.4 are shown the coordinates for some of these special points. The solid circle shows the point, while the open circles indicate points of high symmetry.

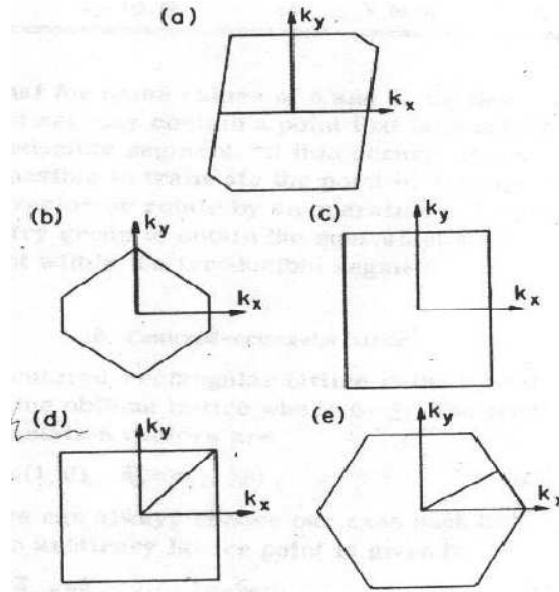


Figure 4.5: Bidimensional Brillouin zones and their irreducible segments for the five types of lattice: oblique, centered rectangular, primitive rectangular, square, and hexagonal, from Cunningham (1974).

II

A year later Cunningham (1974), from the university of California treats the integration around special points in the Brillouin zone. He proposed a more general way of obtaining several sets of special points. From a more general analysis, he obtained the mean value points. In fact, by applying Chadi and Cohen's method for the determination of sets of special wave vectors, for each of the five types of lattice, mean value points, as defined by Baldereschi, have been obtained.

In figure 4.5 Cunningham's method is illustrated.

III

From Salt Lake city we have the work of Monkhorst & Pack (1976), where, in a still more general way, we have a treatment of the special points over the Brillouin zone, and we

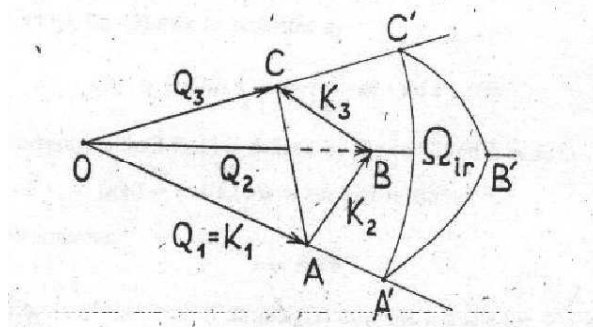


Figure 4.6: Solid angle integrals approximated to integrals over triangles. From Holas (1976).

obtain once more Baldereschi's mean value points. This work shows there is an analytical way to define which points have more weight in the integral, and a relevant example is the mean value point.

IV

From Dubna, later that same year of 1976, we have Holas (1976), an extensive, didactic article in which integrals over solid angle are simplified to integrals over triangles, which is illustrated in figure 4.6, where we can see in which way the solid angle is approximated by a triangle.

V

Froyen (1988) extends the method of Monkhorst & Pack.

He goes farther as to criticize the name “integration by special points”, and proposing the name “Fouier's quadrature” saying that is what we are really doing.

Froyen's extension is for superlattice or supercell geometry, identifying the lattice points that are common for two cells, this minimizing systematic errors.

One of the charms of this article is the summary of the process of selection and generation of Fourier quadrature for Brillouin zone integration.

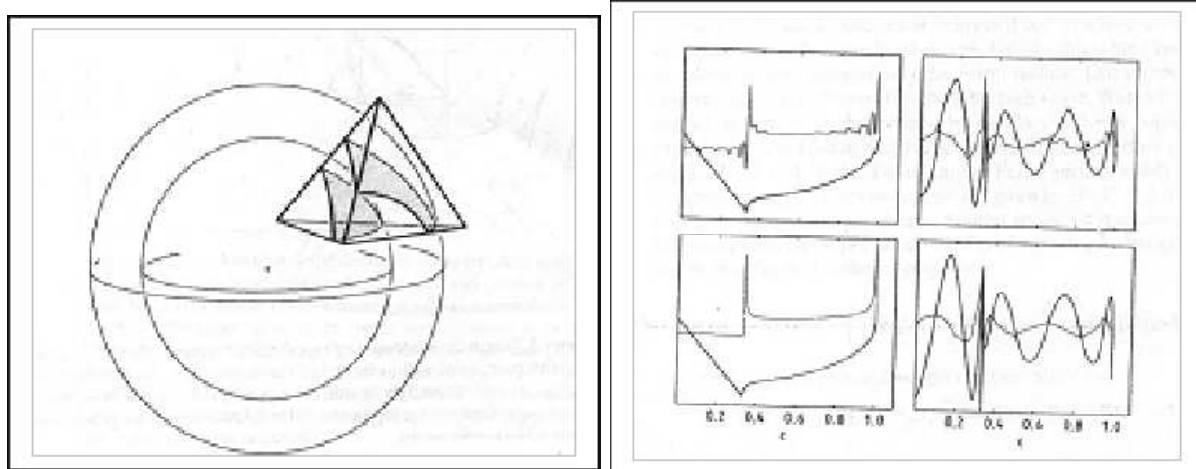


Figure 4.7: Integrals of the Green's functions for the simple cubic tight binding band. The number of tetrahedroes used in the integration is 1728 for the linear case, and 216 in the quadratic case. From Boon, Methfessel & Mueller (1986).

VI

In 1985 we'd have a methodological evolution with Boon, Methfessel & Mueller (1985). In this article the authors propose the analytical quadratic method to evaluate such integrals to obtain the density of states. The main advantage of this method with respect to the linear method, is that the calculation is much simpler and the results just as acceptable.

VII

A year later we'd have Boon, Methfessel & Mueller (1986). Here, the integration over special points was redefined. The integration is performed over tetrahedros, using the analytical quadratic method with a relatively small quantity of tetrahedros. This method is generalized for the density of states for any singular integral. In figure 4.7 are compared the integrals of Green's functions for the simple cubic tight binding band.

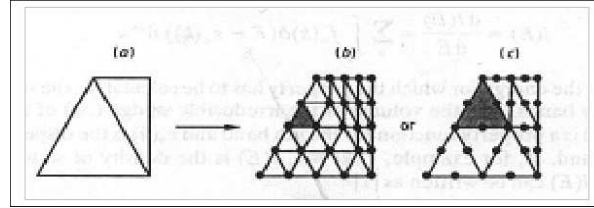


Figure 4.8: k points spaced in irreducible segments. From Wieseneker (1987).

VIII

Wieseneker (1987) is an extension of Boon, Methfessel & Mueller (1986). Here they proceed with an algebraic method instead of the geometric method used by Methfessel. The geometric method described in (Boon, Methfessel & Mueller, 1986) works fine, but due to its geometric nature, an extension to more dimensions is not direct. The algebraic method has no such inconvenience. In figure 4.8 we see an example of the k points spaced in irreducible segments.

IX

An illustrative example of the efforts made to simplify this calculations can be also found in Boerrigter (1988)-

Here, bidimensional integrals are treated as simply as unidimensional integrals. The methodology used to avoid singularities is a coordinate change, from cartesian to spherical, and partitions in “generalized cones”, as it is shown in figure 4.9.

X

Winkler (1993) threw some new light into the problem by saying that the quadratic method of Boon, Methfessel & Mueller (1985, 1986) didn’t weight the points correctly, just like the linear method. Winkler (1993) take into consideration a series of circumstances to obtain this weight factors, as indicated in figure 4.10.

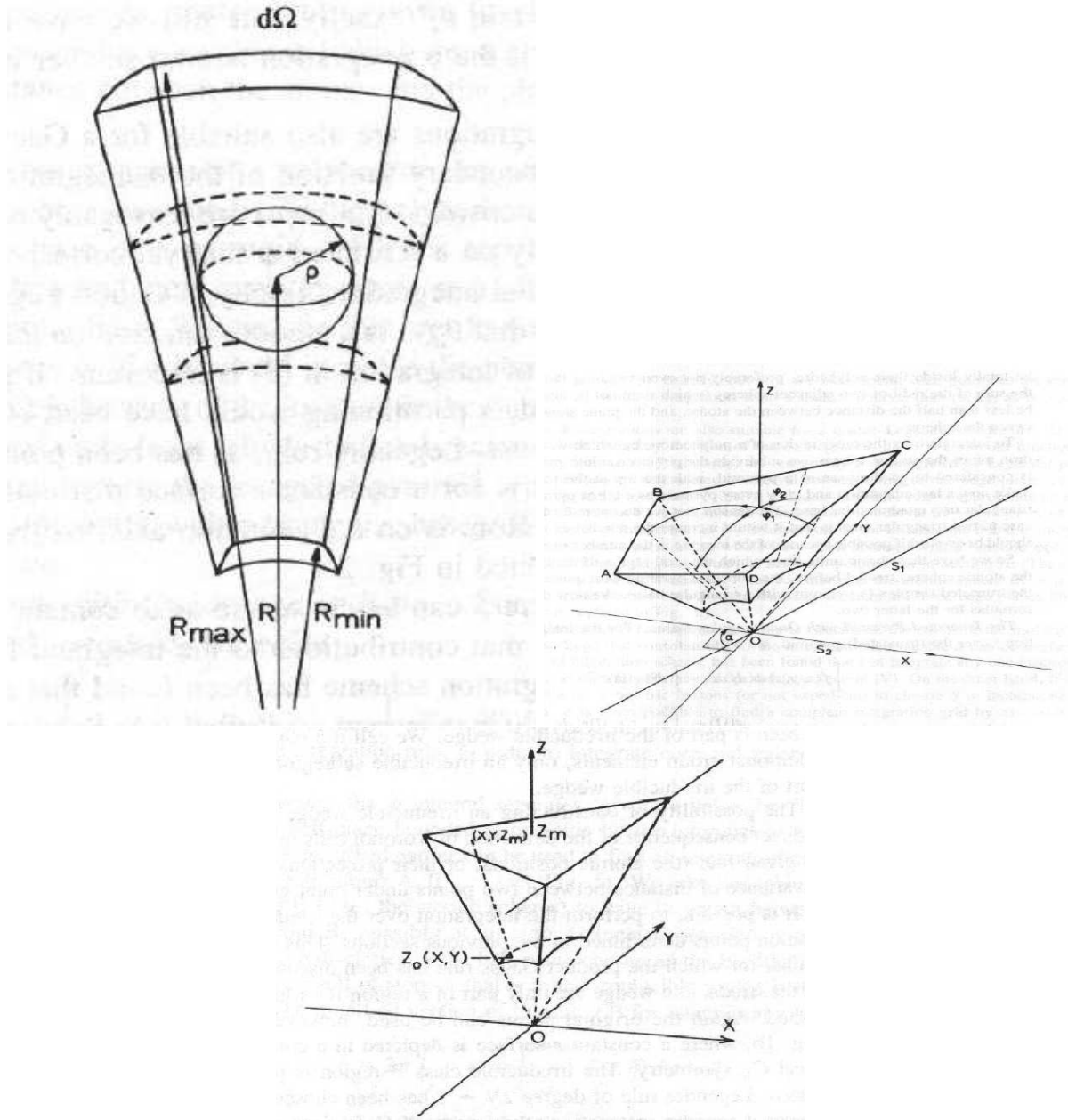


Figure 4.9: Generalized cones of Boerrigter (1988). In the upper left image we show a generalized cone surrounding an atom in position R . The plane has four plane edges. In the upper right figure it is shown an integration region made of a square base pyramid. In the lower figure we can see the integration region consisting of a triangular based pyramid, or “simplex”.

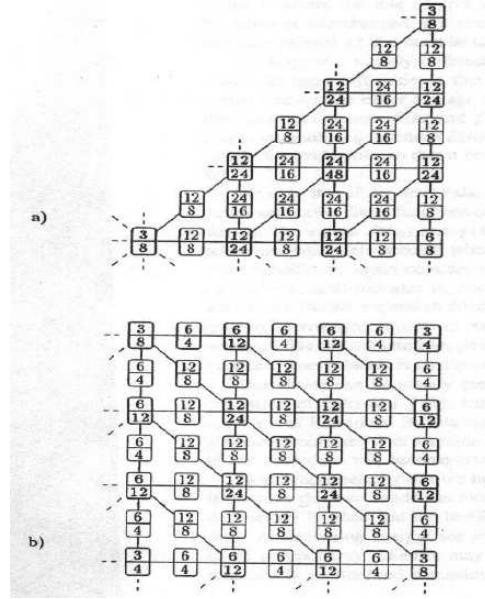


Figure 4.10: The error in the weight factors is shown. In the upper part of each square, we see the factor as considered by Winkler (1993) and in the bottom the one considered by the quadratic interpolation scheme. From Winkler (1993).

XI

Enders (1995) makes a presentation of a numerical method that reduces integration time by paying more attention to band structure than to local details.

Conclusion

It is clear that the integration of singular functions in the Brillouin zone is not a trivial problem, and that many efforts have previously been made to ease this process. Our focus has been to use the MATHEMATICA software for this purpose. Our job is simple, but shines new light on the problem by using modern tools that might turn out to be efficient for this calculations. As we will see in the next chapter, the calculation time isn't too large in the case of 1D, 2D y 3D. If we change the order of calculation between the extraction of the imaginary part part of the function and the integration, it might take

more time, since we need a large number of points to appreciate the error introduced in some of the curves by the changing in this order of calculations.

Chapter 5

Results and Discussion

5.1 1D

In figure 5.1 we show the MATHEMATICA routine we used to calculate the curves shown in figure 5.2. For simplicity we have made $a = E_0 = 1$.

```
integral[j_, s_, nn_, oo_] := Module[{},  
  ListPlot[Table[{e,  $\frac{-1}{\pi}$  Im  
    [NIntegrate[1 / (e + i s - 2 j (Cos[k1]])],  
    {k1, -Pi, Pi}]]}, {e, -20, 20, nn}],  
  PlotJoined → True, AxesLabel → {"E", "DOS"},  
  PlotRange → oo];  
] // Timing
```

Figure 5.1: Routine that calculates the density of states for an infinite chain.

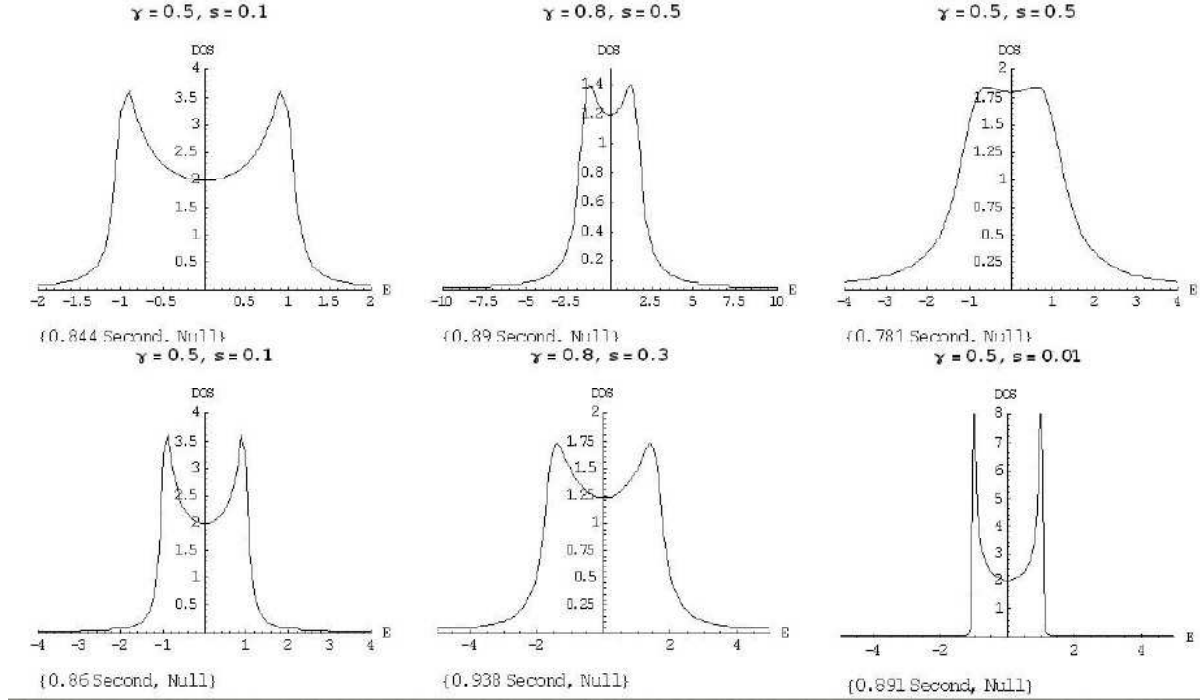


Figure 5.2: Plots of the density of states for an infinite chain with varying parameters.

5.2 2D

For bi-dimensional systems, we have used the code shown in figure 5.3. It is very similar to the one used for one dimension; we have only added another direction in the lattice. Figure 5.4 shows examples of the curves we obtained.

5.3 3D

The routine is shown in figure 5.5 and some curves in figure 5.6.

5.6.

```

integral2[j_, s_, nn_, kk_] := Module[{}, ListPlot[Table[{e,  $\frac{-1}{\pi}$  Im
  [NIntegrate[1/ (e + i s - 2 j (Cos[k1] + Cos[k2]))],
    {k2, -Pi, Pi},
    {k1, -Pi, Pi}]]], {e, -20, 20, nn}],
  PlotJoined → True, PlotRange → kk, AxesLabel → {"E", "DOS"}];
] // Timing

```

Figure 5.3: Routine that calculates the density of states for a square lattice.

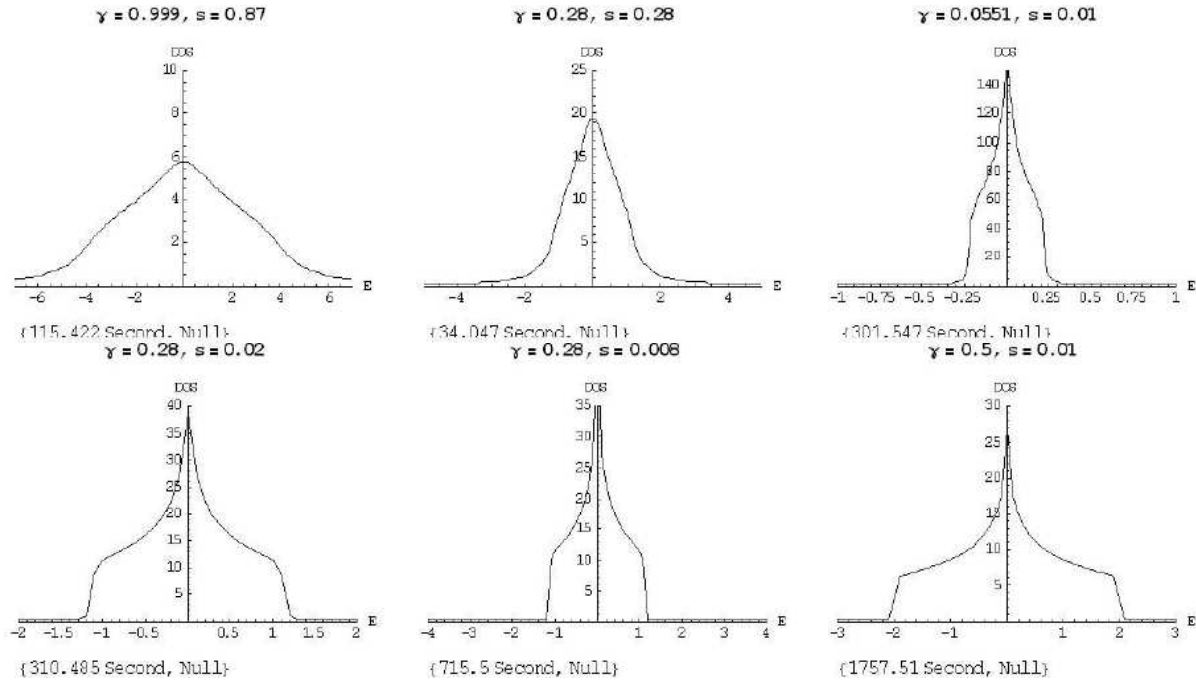


Figure 5.4: Plots of the density of states for a square lattice with varying parameters.

```

tridimbefore[j_, s_, nn_, kk_] := Module[{},
  ListPlot[Table[{e,  $\frac{-1}{\pi}$  Im
    [NIntegrate[1/ (e + i s - 2 j (Cos[k1] + Cos[k2] + Cos[k3]))],
      {k3, -Pi, Pi}, {k2, -Pi, Pi},
      {k1, -Pi, Pi}]]], {e, -20, 20, nn}],
    PlotJoined → True,
    PlotRange → kk, AxesLabel → {"E", "DOS"}];
] // Timing

```

Figure 5.5: Routine that calculates the density of states for a cubical lattice.

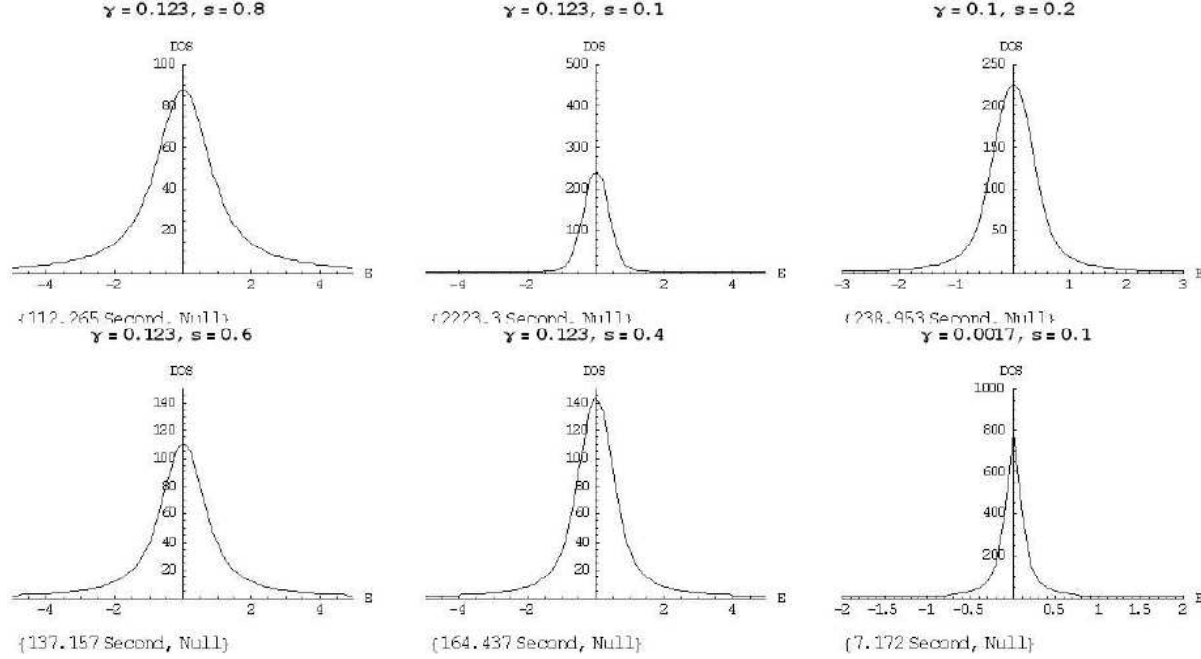


Figure 5.6: Plots of the density of states for a cubical lattice with varying parameters.

5.4 Change of the order of the calculations

Theoretically, the order of the DOS calculations can be swapped. This means we can first extract the imaginary part of the function and then integrate.

In the previous examples first we have integrated the function and then we have separated the imaginary part from the complex function, hoping the internal routines solve themselves the problems that come up when integrating complex functions.

$$D(E) = -\frac{1}{\pi} \Im \int_{-\frac{\pi}{a}}^{\frac{\pi}{a}} G(E + is; k) dk \quad (5.1)$$

Nonetheless, we can also do:

$$D(E) = -\frac{1}{\pi} \int_{-\frac{\pi}{a}}^{\frac{\pi}{a}} \Im G(E + is; k) dk \quad (5.2)$$

For a deeper analysis we compare the curves obtained with the different methods.

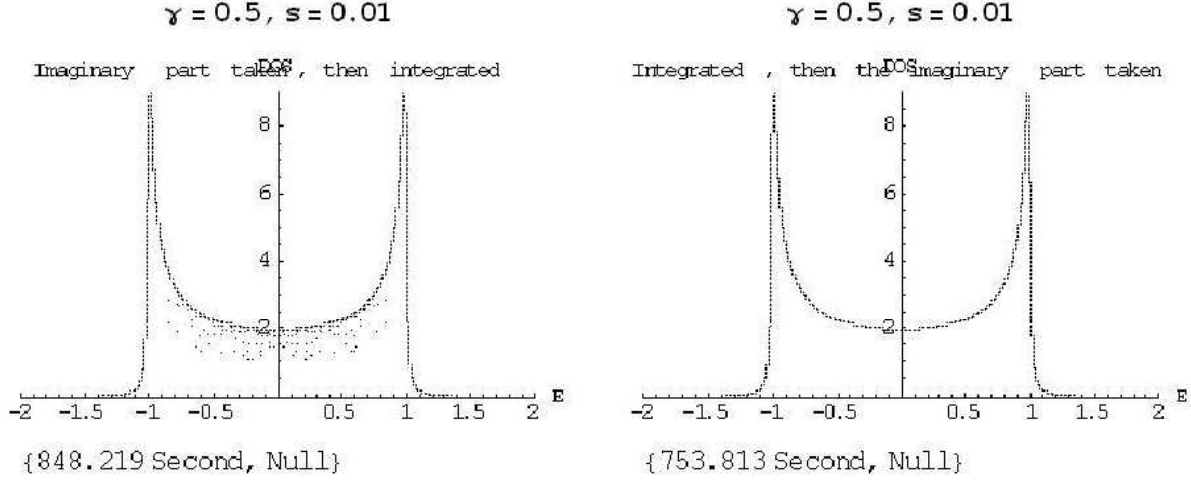


Figure 5.7: Curves we obtained integrating just the imaginary part. We can see some noise that doesn't show when we first integrate and then separate.

In figure 5.7 we can see clearly that for these particular parameters it is better to first integrate and then obtain the imaginary part, as we can see in the left curve, where only the imaginary part was integrated, we get noise in the lower part of the curve. In 2D and 3D we didn't find a situation as clear as the one we show here.

5.5 Conclusion

We conclude the present work noting that we have used a new methodology to calculate the DOS. We can expand this project taking advantage of the simplicity of this method to integrate singular functions in the Brillouin zone, which, as we have seen, is not trivial.

We have deduced the theoretical basis for the computation. We have complemented with an analysis of the literature, and we have also studied the numerical integration provided by MATHEMATICA (with the limitation of the internal routines being secret) and we have concluded with the presentation of the curves obtained for 1D, 2D and 3D crystals.

The following step can be to apply this to calculate the DOS for real materials, besides

we can also try other advanced computation platforms, such as MAPLE.

NOTE: The computations were performed by a machine with a Pentium processor running at 1.70 GHz and 480 MB RAM.

Bibliography

Baldereschi A., 1973, Physical Review, 5212

Beiser A. 1965, Mc Graw Hill

Boerrigter P. M., te Velde G., Baerends E. J., International Journal of Quantum Chemistry, 88

Boon M. H., Methfessel M. S., Mueller F. M., 1985, Journal of Physics C: Solid State Physics, 13, 1012

Boon M. H., Methfessel M. S., Mueller F. M., 1986, Journal of Physics C: Solid State Physics, 20, 1069

Cunningham S. L., 1974, Physical Review B, 10, 4988

Enders P., 1995, Semiconductor Science and Technology 11, 187

Froyen S., 1988, Physical Review B, 39, 3169

Grosso G., Pastori G., 2000, Solid State Physics, Academic Press.

Holas A., Journal of Computational Physics, 23, 151

The Mathematica Guidebooks: Numerical Calculations CD

Monkhorst H. J., Pack J. D., 1976, Physical Review B, 13, 5188

Wieseneker G., te Velde G., Baerends E. J., 1987, Journal of Physics 21 C, 4263

Winkler R., 1993, Journal of Physics Condensed Matter, 2321

Wolfram S., 1991, Mathematica, Addison-Wesley